Development of a Mathematical Model for Vane-type Air Motors with Arbitrary *N* Vanes

Xing Luo, Jihong Wang[1], Leonid Shpanin, Nan Jia, Gang Liu, Alan S. I. Zinober

***Abstract*— The paper presents a mathematical model for vane-type air motors with arbitrary number of vanes. The paper starts from the working principles of the air motor and modeling approach. Then the mechanical geometry structure of air motors is analyzed in order to derive a generic mathematical description of the air motor. A complete dynamic process of the air motor system is derived based on the mechanical structure, orifice and other physics theory. The simulation results are presented with a typical set of air motor parameters. Due to the nature of the motor structure, the chamber volume changes are discontinuous which leads to discontinuous chamber pressure variations. The characteristics of the discontinuity present difficulties for applying advanced control theory to air motor control. Therefore, further approximations are carried out and the comparison of dynamic responses between the original model and the approximated model indicated that the approximation is accurate enough to be acceptable for control strategy development.**

Keywords: pneumatic drives; vane-type air motor; mathematical modelling.

Nomenclature

N	the number of vanes of a vane type air motor
A	effective port width of the control valve
B	radius of motor body
C_0	flow constant = $k\{R[(k+1)/2]^{(k+1)/(k-1)}\}$
C_d	discharge coefficient
C_v	The specific heat of air at constant volume
C_p	The specific heat of air at constant pressure
e	eccentricity (=B-r)
J	inertia of motor
k	ratio of specific heat (for air k=1.4)
L	vane active length in the axial direction
M	drive torque
M_c	stiction coefficient
M_f	friction coefficient
P	pressure
P_{atm}	atmospheric pressure
ρ_r	ratio between downstream and upstream pressure
P_s	supply pressure
P_e	exhust pressure
R	gas constant
r	rotor radius
T	temperature
T_s	supply temperature
X	valve spool displacement
X_a	vane working radius measured from rotor centre
ω	mass flow rate
ϕ	motor rotating angle
V	volume

Subscripts

a	inlet chambers
b	outlet chambers
d	downstream
i	initial condition
u	upstream

I. Introduction

Pneumatic actuators convert the compressed air power energy to the mechanical energy through motion technology. They can be employed extensively for simple position and speed control applications in industry. In the UK, a massive amount of energy, over 10% of the National Grid output, is used to generate compressed air [1]. And also, in 1998, in Japan, pneumatic systems consumed 10% to 20% of the total electricity supplied to factories [2]. That counted approximately up to 5% of the national total electricity consumed in Japan [3]. However, for most precision applications, electrical and hydraulic actuators are widely used due to some difficulties of the pneumatic actuators, especially on the non-linearity and air compressibility [4].

The work is partly supported by EPSRC, UK.

X Luo is with Department of Electronic, Electrical and Computer Engineering, the University of Birmingham, Birmingham, B15 2TT, UK.

N Jia is with Department of Electronic, Electrical and Computer Engineering, the University of Birmingham, Birmingham, B15 2TT, UK.

[1]J Wang is the author for correspondence and is with Department of Electronic, Electrical and Computer Engineering, the University of Birmingham, Birmingham, B15 2TT, UK. Email: j.h.wang@bham.ac.uk.

L Shpanin with Department of Electronic, Electrical and Computer Engineering, the University of Birmingham, Birmingham, B15 2TT, UK.

G Liu is with Department of Applied Mathematics, the University of Sheffield, Sheffield, S10 2TN, UK

A Zinober is with Department of Applied Mathematics, the University of Sheffield, Sheffield, S10 2TN, UK

Air motors, one type of popular pneumatic actuators, are now used in different industrial fields. Compared with its electrical counterpart, air motor systems have some advantages, such as more environmental friendly, simpler in structure, easier in maintenance and safer in operation. The air motors can work in harsh environments, work without sparks, stall without damages, such as food processing, mining industry and etc. For higher precision measurements and further control strategy research, in recent years, some investigative achievements on the study of pneumatic drives and employing pneumatic actuators to accomplish motion control tasks have been obtained [6, 7].

One of the pneumatic actuators, vane type air motors, is introduced in this paper and its mechanical structure and working processes are described in details. A mathematical model of an air motor with four vanes was described in [5]. This study is trying to develop a complete vane-type air motor with *N* vanes. For vane type air motors, the chamber volumes vary in both driving and driven chambers are discontinuous because the number of vanes of an air motor is finite. So the discontinuity of the system model has been discussed and approximated continuous model is derived. Simulation studies are carried out to find out how close the approximated model to the discontinuous model.

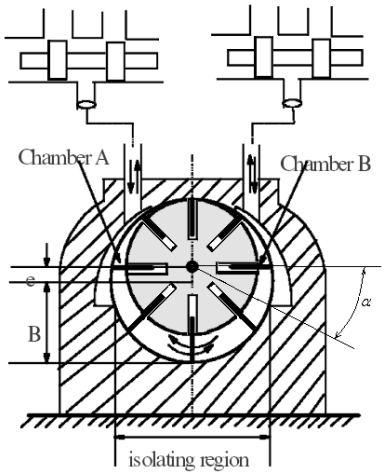

Figure 1 A vane-type air motor with eight vanes and 3-port control valves

II. Working Principles of Vane-Type Air Motors

For studying the vane-type air motor characteristic and developing the air motor dynamic model, a typical vane-type air motor with eight vanes and two 3-port control valves is schematically shown in Figure 1. From the figure, it is clearly seen that a rotating component is a slotted rotor, and it is mounted on a driving shaft. Each slot of the rotor is fitted with a freely sliding rectangular vane. So the vane type air motor with eight vanes means that there has 45 degrees between any two rectangular vanes on the rotor. When the rotor is in motion, the vanes tend to slide outward as centrifugal force. The vane in the isolating region divides the control volume inside the air motor into two parts, Chamber A and Chamber B with eight sections which are inside the air motor and are divided by the vanes as shown in Figure 2.

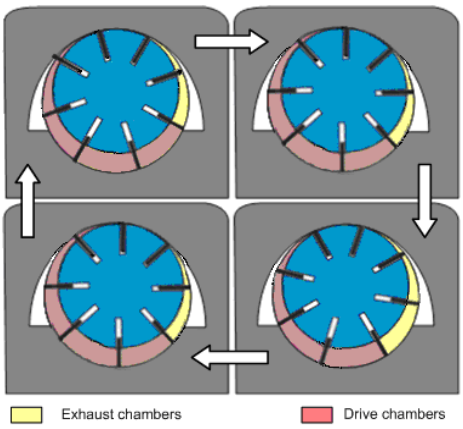

Figure 2 Schematic diagram of a vane-type air motor in motion

The difference of air pressure provides forces on the vanes, so the motor can rotate in either direction [8]. For instance, if the one port on Chamber A connects to the air supply, another port opens to atmosphere. In that case, the air pressure in Chamber A (driving chamber) is greater than that in Chamber B (driven chambers), so the motor rotates in the way of anticlockwise and the rotor turns continuously. A schematic diagram of a vane-type air motor with eight vanes in anticlockwise rotation is illustrated in Figure 2. The force by compressed air due to the difference of pressures in the two chambers drives the rotor rotation. That means the potential energy of the compressed air is converted into the kinetic energy of the rotor and torques.

III. Dynamic Model of Air Motor System

A dynamic model of an air motor with *N* vanes is investigated in this section. The derivation of the volumes of driving and driven chambers, dynamic relationship within the control chambers and the pressure variation of the air motor system are studied in depth.

3.1 The volumes of driving and driven chambers

A simplified vane type air motor is shown in Figure 3. Based on its structure, the volumes of driving and driven chambers can be derived as follows. Assuming that the pressure in the isolated volume is the same as the pressure in the driving chamber and the volume of each isolated chamber is the same. So the isolated volume belongs to the driving chamber. And assume that the balance position of the motor rotation is at $\phi = 0$. The volumes of the driving and driven chambers are described individually by

$$V_a(0) = \frac{1}{2} L(B^2 - r^2)\pi + V_n \qquad (3.1)$$

$$V_b(0)=\frac{1}{2}L(B^2-r^2)\pi-V_n \tag{3.2}$$

where, V_n is the half volume of all of the isolated chambers at the balance position. If $\frac{2\pi}{N}>\frac{\pi}{2}-\alpha$, V_n=0.

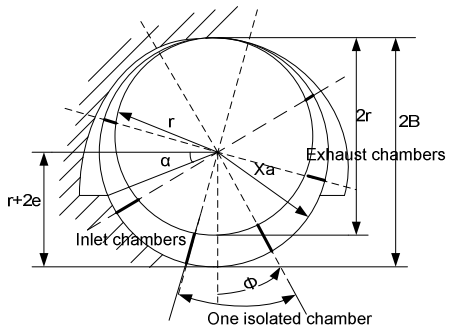

Figure 3 Vane-type air motor structure

Assume the volume of one isolated chamber is V_m.

$$V_n=\frac{1}{2}V_m\times roundoff\,[\frac{(\pi-2\alpha)}{2\pi/N}] \tag{3.3}$$

The *roundoff* stands for integer part of $[\frac{(\pi-2\alpha)}{(2\pi/N)}]$.

The vane working radius X_a is

$$x_a=e\cos\phi+\sqrt{B^2-e^2\sin^2\phi} \tag{3.4}$$

When the rotation direction is anticlockwise and suppose that $e^2\sin^2\phi<<B^2$, the control volume of the driving and driven chambers are described respectively by

$$V_a=\frac{1}{2}L(B^2-r^2)[\pi+(\phi-j\frac{2\pi}{N})]+\frac{1}{4}Le^2\sin 2(\phi-j\frac{2\pi}{N})$$
$$+LBe\sin(\phi-j\frac{2\pi}{N})+\frac{1}{4}L[\frac{e^2}{2}\sin(\frac{4\pi}{N})+2eB\sin(\frac{2\pi}{N})+B^2(\frac{2\pi}{N})$$
$$-r^2(\frac{2\pi}{N})]\times roundoff[\frac{(\pi-2\alpha)}{2\pi/N}] \tag{3.5}$$

$$V_b=\frac{1}{2}L(B^2-r^2)[\pi-(\phi-j\frac{2\pi}{N})]-\frac{1}{4}Le^2\sin 2(\phi-j\frac{2\pi}{N})$$
$$-LBe\sin(\phi-j\frac{2\pi}{N})-\frac{1}{4}L[\frac{e^2}{2}\sin(\frac{4\pi}{N})+2eB\sin(\frac{2\pi}{N})+B^2(\frac{2\pi}{N})$$
$$-r^2(\frac{2\pi}{N})]\times roundoff[\frac{(\pi-2\alpha)}{2\pi/N}] \tag{3.6}$$

where $\phi\in[-\alpha+j\frac{2\pi}{N},-\alpha+(j+1)+\frac{2\pi}{N}],\ j=0,\pm1,\pm2,...$

The derivative of V_a and V_b are

$$\frac{dV_a}{dt}=\frac{dV_a}{d\phi}\cdot\frac{d\phi}{dt}=\tilde{V}_a\cdot\frac{d\phi}{dt}$$

and $$\frac{dV_b}{dt}=\frac{dV_b}{d\phi}\cdot\frac{d\phi}{dt}=\tilde{V}_b\cdot\frac{d\phi}{dt}$$

with

$$\tilde{V}_a=\frac{1}{2}L\cdot[(B^2-r^2)+e^2\cos 2(\phi-j\frac{2\pi}{N})+2Be\cos(\phi-j\frac{2\pi}{N}) \tag{3.7}$$

and $$\tilde{V}_b=-\tilde{V}_a \tag{3.8}$$

Based on (3.5) to (3.8), V_a,V_b,$\tilde{V}_a$ and $\tilde{V}_b$ are periodic and discontinuous (assume the number of vanes is finite) functions.

When Chamber B is the driving chamber, i.e. the rotor turns anticlockwise,

$$V_a=\frac{1}{2}L(B^2-r^2)[\pi+(\phi-(j+1)\frac{2\pi}{N})]+\frac{1}{4}Le^2\sin 2(\phi-(j+1)\frac{2\pi}{N})$$
$$+LBe\sin(\phi-(j+1)\frac{2\pi}{N})-\frac{1}{4}L[\frac{e^2}{2}\sin(\frac{4\pi}{N})+2eB\sin(\frac{2\pi}{N})+B^2(\frac{2\pi}{N})$$
$$-r^2(\frac{2\pi}{N})]\times roundoff[\frac{(\pi-2\alpha)}{2\pi/N}] \tag{3.9}$$

$$V_b=\frac{1}{2}L(B^2-r^2)[\pi-(\phi-(j+1)\frac{2\pi}{N})]-\frac{1}{4}Le^2\sin 2(\phi-(j+1)\frac{2\pi}{N})$$
$$-LBe\sin(\phi-(j+1)\frac{2\pi}{N})+\frac{1}{4}L[\frac{e^2}{2}\sin(\frac{4\pi}{N})+2eB\sin(\frac{2\pi}{N})+B^2(\frac{2\pi}{N})$$
$$-r^2(\frac{2\pi}{N})]\times roundoff[\frac{(\pi-2\alpha)}{2\pi/N}] \tag{3.10}$$

and $$\tilde{V}_b=-\tilde{V}_a \tag{3.11}$$

The analysis of the dynamic characteristic of a pneumatic system normally includes three individual mathematical functions of its components, i.e. the valve, the actuator and the load [5, 9, 10].

3.2 Flow relationships of the control valves

Assume the constant supply pressure and exhaust pressure, the mass flow rates across the control valves can be described by [10]

$$w=q(X,P) \tag{3.12}$$

Based on the standard orifice theory [10, 11], the mass flow rate through the valve orifice takes form

$$w=C_dC_0AXP_u\overline{f}(p_r)/\sqrt{T_u} \tag{3.13}$$

where $p_r=P_d/P_u$ is ratio between the downstream and upstream pressures at the orifice and

$$\tilde{f}(p_r)\begin{cases}1 & \frac{P_{atm}}{P_s}\le p_r\le C_r\\ C_k\left[p_r^{2/\gamma}-p_r^{(\gamma+1)/\gamma}\right]^{1/2} & C_r<p_r\le 1\end{cases} \tag{3.14}$$

For air k =1.4, C_r = 0.528 and C_k = 3.864. So the function $\tilde{f}(\cdot)$ and its derivative are continuous.

For the simplified calculation of the mass flow rate through the valves, the following functions are introduced

For chamber A

$$f(P_a,P_s,P_e)=\begin{cases} P_s\tilde{f}\left(\frac{P_a}{P_s}\right)\Big/\sqrt{T_s} & \text{Chamber A is the drive chamber} \\ P_a\tilde{f}\left(\frac{P_e}{P_a}\right)\Big/\sqrt{T_a} & \text{Chamber B is the drive chamber} \end{cases}$$

For chamber B

$$f(P_b,P_s,P_e)=\begin{cases} P_b\tilde{f}\left(\frac{P_e}{P_b}\right)\Big/\sqrt{T_b} & \text{Chamber A is the drive chamber} \\ P_s\tilde{f}\left(\frac{P_b}{P_s}\right)\Big/\sqrt{T_s} & \text{Chamber B is the drive chamber} \end{cases}$$

3.3 Pressure relationships in the control chambers

The formula of the mass flow rate can utilize [10, 12],

$$w=(\frac{P\dot{V}+\dot{P}V}{k})/(RT_s) \tag{3.15}$$

The dynamic relationship of the pressure of the motor within the driving and driven chambers can be described by

$$\dot{P}_a=\frac{kRT_sC_dC_0A_aX_af(P_a,P_s,P_e)}{V_a}-\frac{kP_a}{V_a}\frac{dV_a}{d\phi}\frac{d\phi}{dt} \tag{3.16}$$

$$\dot{P}_b=\frac{kRT_sC_dC_0A_bX_bf(P_b,P_s,P_e)}{V_b}-\frac{kP_b}{V_b}\frac{dV_b}{d\phi}\frac{d\phi}{dt} \tag{3.17}$$

3.4 Load dynamics

The pneumatic system should consider its friction and payloads. Based on Newton's second law of angular motion [12],

$$M-M_cS\left(\dot{\phi}\right)-M_f\dot{\phi}=J\ddot{\phi} \tag{3.18}$$

where $\dot{\phi}$ is angular velocity, $\ddot{\phi}$ is angular acceleration, and $S\left(\dot{\phi}\right)$ can be calculated by

$$S\left(\dot{\phi}\right)=\begin{cases} 1, & \dot{\phi}=0 \\ sign\left(\dot{\phi}\right)\partial_c \quad (0\le\partial_c<1) & \dot{\phi}\ne 0 \end{cases} \tag{3.19}$$

The drive torque depends on the force by the difference of the pressure between the drive and exhaust chambers (see Figure 4). It acts on a part area of the vane which one side is the drive chambers and another side is the exhaust chambers.

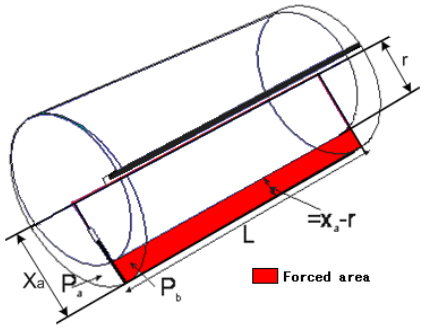

Figure 4 Schematic diagram of the forced area on a vane

So the drive torque is described by

$$\begin{aligned} M&=(P_a-P_b)\times(x_a^2-r^2)\frac{L}{2} \\ &=(P_a-P_b)\times(e^2\cos 2\phi+2eB\cos\phi+B^2-r^2)\frac{L}{2} \end{aligned} \tag{3.20}$$

According to equation (3.20), the angular acceleration $\ddot{\phi}$ of the motor can be described by

$$\begin{aligned} \ddot{\phi}=&\frac{L}{2J}(P_a-P_b)\times(e^2\cos 2\phi+2eB\cos\phi+B^2-r^2) \\ &-\frac{M_c}{J}S\left(\dot{\phi}\right)-\frac{M_f}{J}\dot{\phi} \end{aligned} \tag{3.21}$$

Form equations (3.16) to (3.21), the state functions of the vane type air motor with *N* vanes can be derived. The state variables are chosen to

be $x_1=\phi, x_2=\dot{\phi}, x_3=P_a, x_4=P_b$, and the control input variables $u_1=X_a, u_2=X_b$. Then the state functions of the N vanes air motor can be described as follows:

$$\dot{x}_1(t)=x_2(t)$$

$$\begin{aligned} \dot{x}_2(t)=&\frac{L}{2J}(x_3-x_4)\times(e^2\cos 2x_1+2eB\cos x_1+B^2-r^2) \\ &-\frac{M_c}{J}S(x_2)-\frac{M_f}{J}x_2 \end{aligned}$$

$$\dot{x}_3(t)=\frac{kRT_sC_dC_0A_au_1(t)f(x_3(t),P_s,P_e)}{V_a(x_1(t))}-\frac{k}{V_a(x_1(t))}\frac{dV_a(x_1(t))}{dx_1(t)}x_3(t)x_2(t)$$

$$\dot{x}_4(t)=\frac{kRT_sC_dC_0A_bu_2(t)f(x_4(t),P_s,P_e)}{V_b(x_1(t))}-\frac{k}{V_b(x_1(t))}\frac{dV_b(x_1(t))}{dx_1(t)}x_2(t)x_4(t)$$

IV. SIMULATION STUDY

The system model parameters are given as follows for the simulation study:
M_c=0.5N, M_f=0.09Ns, L=44.5mm, B=36.5mm, e=4mm, $r=B-e$, J_1=6.08×10-4 kgm^2, J_2=2.69×10-4 kgm^2, $J=J_1+J_2$, T_s=293K, P_s=6 bar, $\alpha=\pi/6$, k=1.4, C_d=0.8 C_0=0.0404, A_a=A_b=0.003m, R=287J(kgK)$^{-1}$

According to the state functions of the vane type air motor with *N* vanes and the model's parameters as above, a vane-type air motor model was implemented in Simulink.

Assume the rotor now turns in the way of anticlockwise, i.e. Chamber A stands for driving chamber and Chamber B stands for driven chamber (see Figure 1). The simulation results are shown in Figures 5 ~ 8.

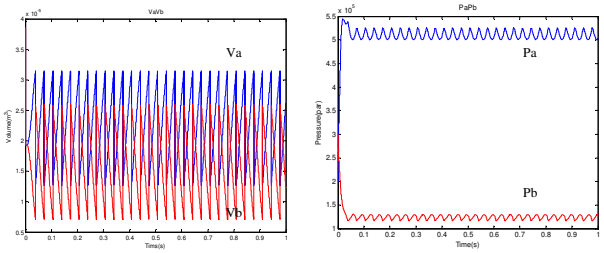

Figure 5 Simulation results of vane motor dynamic model (N=4)

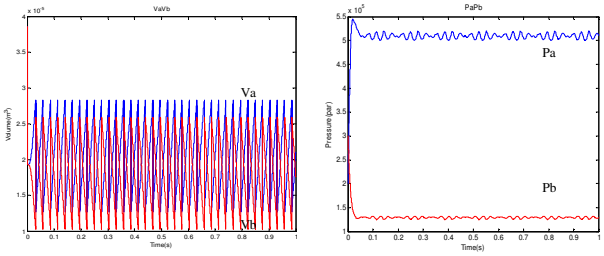

Figure 6 Simulation results of vane motor dynamic model (N=5)

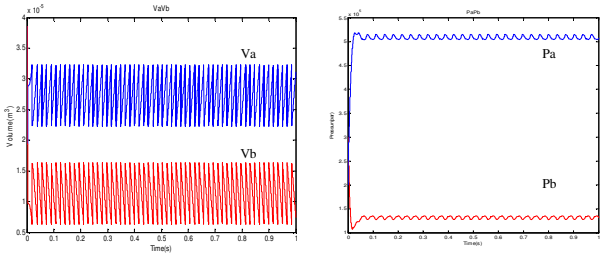

Figure 7 Simulation results of vane motor dynamic model (N=8)

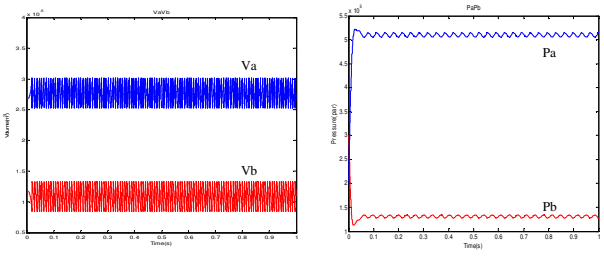

Figure 8 Simulation results of vane motor dynamic model (N=16)

Figure 5 to Figure 8, show the pressure variation within the chambers for the cases that the number of vanes (N) equals to 4, 5, 8, and 16 separately. Based on the figures, the maximum volume of drive chambers changes from $2.73\times10^{-5}m^3$ to $3.81\times10^{-5}m^3$. And the maximum volume of exhaust chambers change from $1.31\times10^{-5}m^3$ to $2.59\times10^{-5}m^3$. From Figure 5 to Figure 8, it is shown that after a short initial time, the control volume variation and the pressure variation are periodic and the frequency depends on the number of vanes of the air motor. From the figures, the responses are smoother when the number of vanes increases.

V. CONTINUOUS APPROXIMATION TO CHAMBER VOLIMES

The discontinuities of V_a, V_b, $\tilde{V}_a$ and $\tilde{V}_b$ could lead to difficulties for applying control theory. Thus, a *Fourier* series expansion is employed to obtain the continuous form of V_a, V_b, $\tilde{V}_a$ and $\tilde{V}_b$. The *Fourier* series expansions of V_a, V_b, $\tilde{V}_a$ and $\tilde{V}_b$ can be described by:

$$V_a = \frac{a_{a0}}{2} + \sum_{n=1}^{\infty} a_{an}\cos(Nn\phi) + \sum_{n=1}^{\infty} b_{an}\sin(Nn\phi) \tag{5.1}$$

$$V_b = \frac{a_{b0}}{2} + \sum_{n=1}^{\infty} a_{bn}\cos(Nn\phi) + \sum_{n=1}^{\infty} b_{bn}\sin(Nn\phi) \tag{5.2}$$

$$\tilde{V}_a = \frac{\tilde{a}_{a0}}{2} + \sum_{n=1}^{\infty} \tilde{a}_{an}\cos(Nn\phi) + \sum_{n=1}^{\infty} \tilde{b}_{an}\sin(Nn\phi) \tag{5.3}$$

$$\tilde{V}_b = -\tilde{V}_a = -\frac{\tilde{a}_{a0}}{2} - \sum_{n=1}^{\infty} \tilde{a}_{an}\cos(Nn\phi) - \sum_{n=1}^{\infty} \sin\tilde{b}_{an}(Nn\phi) \tag{5.4}$$

where the coefficients $a_{a0}, a_{b0}, a_{an}, a_{bn}, b_{an}, b_{bn}, \tilde{a}_{a0}$, $\tilde{a}_{an}, \tilde{b}_{an}$ are listed in the Appendix. Utilizing Equation (5.1) to Equation (5.4), substitute V_a, V_b, $\tilde{V}_a$ and $\tilde{V}_b$ in the state functions of the vane-type air motor with arbitrary N vanes. Thus, a continuously approximated system model can be obtained.

The coefficient for the Fourier series expansion of $V_a, V_b, \tilde{V}_a, \tilde{V}_b$ are listed below.

$$\begin{aligned} a_{a0} = {} & \pi L(B^2 - r^2) + (\frac{1}{2N}(L(B^2 - r^2)\cdot(N\pi - 2\alpha N - 2\pi))) \\ & + (\frac{N}{\pi}(-\frac{1}{8}\cos(2(\alpha\pi + 2\pi)/N)\cdot Le^2 + \frac{1}{8}Le^2\cos(2\alpha))) \\ & + (\frac{N}{\pi}\cdot(-LBe\sin\alpha + \sin((\alpha N + 2\pi)/N)\cdot LBe)) + \{\frac{N}{\pi}\cdot\frac{1}{4}L \\ & \cdot[\frac{e^2}{2}\sin(\frac{4\pi}{N}) + 2eB\sin(\frac{2\pi}{N}) + B^2(\frac{2\pi}{N}) - r^2(\frac{2\pi}{N})] \\ & \cdot roundoff\,[\frac{(\pi - 2\alpha)}{2\pi/N}]\cdot\frac{2\pi}{N}\} \end{aligned}$$

$$\begin{aligned} a_{b0} = {} & \pi L(B^2 - r^2) - (\frac{1}{2N}(L(B^2 - r^2)\cdot(N\pi - 2\alpha N - 2\pi))) \\ & - (\frac{N}{\pi}(-\frac{1}{8}\cos(2(\alpha\pi + 2\pi)/N)\cdot Le^2 + \frac{1}{8}Le^2\cos(2\alpha))) \\ & - (\frac{N}{\pi}\cdot(-LBe\sin\alpha + \sin((\alpha N + 2\pi)/N)\cdot LBe)) - \{\frac{N}{\pi}\cdot\frac{1}{4}L \end{aligned}$$

$$\cdot[\frac{e^2}{2}\sin(\frac{4\pi}{N})+2eB\sin(\frac{2\pi}{N})+B^2(\frac{2\pi}{N})-r^2(\frac{2\pi}{N})]$$
$$\cdot roundoff[\frac{(\pi-2\alpha)}{2\pi/N}]\cdot\frac{2\pi}{N}\}$$

$$a_{an}=\frac{1}{2}\cdot\frac{N}{\pi}\cdot\frac{L(B^2-r^2)\pi}{Nn}\cdot(\sin(Nn(\frac{\pi}{2}-\alpha))-\sin(Nn(\frac{\pi}{2}-\alpha-\frac{2\pi}{N})))+$$
$$\frac{1}{2}\cdot\frac{N}{\pi}\cdot\frac{L(B^2-r^2)}{N^2n^2}\cdot[(Nn(\frac{\pi}{2}-\alpha)\cdot\sin(Nn(\frac{\pi}{2}-\alpha))+\cos(Nn(\frac{\pi}{2}-\alpha)))$$
$$-(Nn(\frac{\pi}{2}-\alpha-\frac{2\pi}{N})\cdot\sin(Nn(\frac{\pi}{2}-\alpha-\frac{2\pi}{N}))-\cos(Nn(\frac{\pi}{2}-\alpha-\frac{2\pi}{N})))]$$
$$-\frac{1}{8}\cdot\frac{N}{\pi}Le^2[\frac{1}{Nn+2}\cos((Nn+2)(\frac{\pi}{2}-\alpha))-\frac{1}{Nn-2}\cos((Nn-2)(\frac{\pi}{2}-\alpha))$$
$$-\frac{1}{Nn+2}\cos((Nn+2)(\frac{\pi}{2}-\alpha-\frac{2\pi}{N}))+\frac{1}{Nn-2}\cos((Nn-2)(\frac{\pi}{2}-\alpha-\frac{2\pi}{N}))]$$
$$-\frac{1}{2}\cdot\frac{N}{\pi}\cdot LBe[\frac{1}{Nn+1}\cos((Nn+1)(\frac{\pi}{2}-\alpha))-\frac{1}{Nn-1}\cos((Nn-1)(\frac{\pi}{2}-\alpha))$$
$$-\frac{1}{Nn+1}\cos((Nn+1)(\frac{\pi}{2}-\alpha-\frac{2\pi}{N}))+\frac{1}{Nn-1}\cos((Nn-1)(\frac{\pi}{2}-\alpha-\frac{2\pi}{N}))]$$
$$+\{\frac{N}{\pi}\cdot\frac{1}{4}L\cdot[\frac{e^2}{2}\sin(\frac{4\pi}{N})+2eB\sin(\frac{2\pi}{N})+B^2(\frac{2\pi}{N})-r^2(\frac{2\pi}{N})]\cdot roundoff[\frac{(\pi-2\alpha)}{2\pi/N}]$$
$$\cdot[\frac{1}{Nn}\sin(Nn(\frac{\pi}{2}-\alpha))-\frac{1}{Nn}\sin(Nn(\frac{\pi}{2}-\alpha-\frac{2\pi}{N}))]\}$$

$$a_{bn}=-a_{an}$$

$$b_{an}=-\frac{1}{2}\cdot\frac{N}{\pi}\cdot\frac{L(B^2-r^2)\pi}{Nn}\cdot(\cos(Nn(\frac{\pi}{2}-\alpha))-\cos(Nn(\frac{\pi}{2}-\alpha-\frac{2\pi}{N})))+$$
$$\frac{1}{2}\cdot\frac{N}{\pi}\cdot\frac{L(B^2-r^2)}{N^2n^2}\cdot[-(Nn(\frac{\pi}{2}-\alpha)\cdot\cos(Nn(\frac{\pi}{2}-\alpha))+\sin(Nn(\frac{\pi}{2}-\alpha)))$$
$$+(Nn(\frac{\pi}{2}-\alpha-\frac{2\pi}{N})\cdot\cos(Nn(\frac{\pi}{2}-\alpha-\frac{2\pi}{N}))-\sin(Nn(\frac{\pi}{2}-\alpha-\frac{2\pi}{N})))]$$
$$-\frac{1}{8}\cdot\frac{N}{\pi}Le^2[\frac{1}{Nn+2}\sin((Nn+2)(\frac{\pi}{2}-\alpha))-\frac{1}{Nn-2}\sin((Nn-2)(\frac{\pi}{2}-\alpha))$$
$$-\frac{1}{Nn+2}\sin((Nn+2)(\frac{\pi}{2}-\alpha-\frac{2\pi}{N}))+\frac{1}{Nn-2}\sin((Nn-2)(\frac{\pi}{2}-\alpha-\frac{2\pi}{N}))]$$
$$-\frac{1}{2}\cdot\frac{N}{\pi}\cdot LBe[\frac{1}{Nn+1}\sin((Nn+1)(\frac{\pi}{2}-\alpha))-\frac{1}{Nn-1}\sin((Nn-1)(\frac{\pi}{2}-\alpha))$$
$$-\frac{1}{Nn+1}\sin((Nn+1)(\frac{\pi}{2}-\alpha-\frac{2\pi}{N}))+\frac{1}{Nn-1}\sin((Nn-1)(\frac{\pi}{2}-\alpha-\frac{2\pi}{N}))]$$
$$-\{\frac{N}{\pi}\cdot\frac{1}{4}L\cdot[\frac{e^2}{2}\sin(\frac{4\pi}{N})+2eB\sin(\frac{2\pi}{N})+B^2(\frac{2\pi}{N})-r^2(\frac{2\pi}{N})]\cdot roundoff[\frac{(\pi-2\alpha)}{2\pi/N}]$$
$$\cdot[\frac{1}{Nn}\cos(Nn(\frac{\pi}{2}-\alpha))-\frac{1}{Nn}\cos(Nn(\frac{\pi}{2}-\alpha-\frac{2\pi}{N}))]\}$$

$$b_{bn}=-b_{an}$$

$$\tilde{a}_{a0}=L(B^2-r^2)+(\frac{N}{\pi}\cdot(-\frac{1}{4}\sin(2\cdot((\alpha\pi+2\pi)/N))Le^2+$$
$$+\frac{1}{4}\sin(2\alpha)\cdot Le^2))+(\frac{N}{\pi}\cdot(LBe\cos\alpha))-\cos((\alpha\pi+2\pi)/N)LBe))$$

$$\tilde{a}_{an}=\frac{1}{2}\cdot\frac{N}{\pi}\cdot\frac{L(B^2-r^2)}{Nn}\cdot(\sin(Nn(\frac{\pi}{2}-\alpha))-\sin(Nn(\frac{\pi}{2}-\alpha-\frac{2\pi}{N})))+$$
$$+(\frac{N}{\pi}\cdot\frac{1}{4}Le^2(\frac{1}{Nn+2}\cdot\sin((Nn+2)(\frac{\pi}{2}-\alpha))+$$
$$\frac{1}{Nn-2}\cdot\sin((Nn-2)(\frac{\pi}{2}-\alpha))-\frac{1}{Nn+2}\cdot\sin((Nn+2)(\frac{\pi}{2}-\alpha-\frac{2\pi}{N}))$$
$$-\frac{1}{Nn-2}\cdot\sin((Nn-2)(\frac{\pi}{2}-\alpha-\frac{2\pi}{N}))))$$
$$+(\frac{N}{\pi}\cdot\frac{1}{2}LBe(\frac{1}{Nn+1}\cdot\sin((Nn+1)(\frac{\pi}{2}-\alpha))+$$
$$\frac{1}{Nn-1}\cdot\sin((Nn-1)(\frac{\pi}{2}-\alpha))-\frac{1}{Nn+1}\cdot\sin((Nn+1)(\frac{\pi}{2}-\alpha-\frac{2\pi}{N}))$$
$$-\frac{1}{Nn-1}\cdot\sin((Nn-1)(\frac{\pi}{2}-\alpha-\frac{2\pi}{N}))))$$

$$\tilde{b}_{an}=-\frac{1}{2}\cdot\frac{N}{\pi}\cdot\frac{L(B^2-r^2)}{Nn}\cdot(\cos(Nn(\frac{\pi}{2}-\alpha))-\cos(Nn(\frac{\pi}{2}-\alpha-\frac{2\pi}{N})))+$$
$$-(\frac{N}{\pi}\cdot\frac{1}{4}Le^2(\frac{1}{Nn+2}\cdot\cos((Nn+2)(\frac{\pi}{2}-\alpha))+$$
$$\frac{1}{Nn-2}\cdot\cos((Nn-2)(\frac{\pi}{2}-\alpha))-\frac{1}{Nn+2}\cdot\cos((Nn+2)(\frac{\pi}{2}-\alpha-\frac{2\pi}{N}))$$
$$-\frac{1}{Nn-2}\cdot\cos((Nn-2)(\frac{\pi}{2}-\alpha-\frac{2\pi}{N}))))$$
$$-(\frac{N}{\pi}\cdot\frac{1}{2}LBe(\frac{1}{Nn+1}\cdot\cos((Nn+1)(\frac{\pi}{2}-\alpha))+$$
$$\frac{1}{Nn-1}\cdot\cos((Nn-1)(\frac{\pi}{2}-\alpha))-\frac{1}{Nn+1}\cdot\cos((Nn+1)(\frac{\pi}{2}-\alpha-\frac{2\pi}{N}))$$
$$-\frac{1}{Nn-1}\cdot\cos((Nn-1)(\frac{\pi}{2}-\alpha-\frac{2\pi}{N}))))$$

Simulation studies revealed that the approximation is accurate enough to represent the true volumes.

VI. Concluding Remarks

In this paper, a complete mathematical model for vane type air motor with an arbitrary number of vanes was developed. The continuous approximation provide control engineers a continuous working model to develop control strategy using modern/advance control methods.

References

[1] Saving Energy in Compressed Air Systems, April 2003, Accessed on: 27 March 2007, Available: *www. energyinst.org.uk/content/files/cpd/compressedair.pdf*

[2] Cai, M, Kawashima, K, Kagawa, T, Power assessment of flowing compressed air, *Journal of Fluid Engineering*, vol. 128, March, pp402-405, 2006.

[3] Cai, M, Kagawa, T, Energy consumption assessment of pneumatic actuating systems including compressor, *IMechE*, pp381-380, 2001.

[4] Wang, J., Pu, J. Moore, P.R.m Zhang, Z., Modelling study and servo-control of air motor systems, *Int. J. Contorl*, vol. 71, No.3, pp459-476, 1998.

[5] Andersen, B.W., *The Analysis and Design of Pneumatic Systems*, New York: Robert E. Krieger Publishing Co. 1976.

[6] Wang, J., Pu, J., Moore, P.R., Accurate position control for pneumatic actuator systems and application to food packaging, *Control Engineering Practice*, Vol. 7, pp699-706, 1999.

[7] Wang, J., Pu, J. and Moore, P.R., A practicable control strategy for servo pneumatic actuator systems, *Control Engineering Practice,* Vol. 7, pp1483-1488, 1999.

[8] HSE Book, *A guide to the Work in Compressed Air Regulations*, 1996

[9] Anthony, D., Control systems for pneumatic sequential machines, University of Birmignham, 1975.

[10] Blackburn, J. F., Beethof, G., and Shearer, J. L., *Fluid Power Control*, New York, The Technology Pree and J. Wiley,

[11] Harris, E.G., *Compressed Air- Theory and Computations*, McGraw-Hill, New York, 2007.

[12] Marion, J. and Thornton, S, *Classical Dynamics of Particles and Systems*, Harcourt College Publishers, 1995.